Supplementary Figure Legends

Fig. S1. PQBP1 and WBP11 sequence comparisons. A. Alignment of PQBP1 protein sequences of human *(Homo sapiens, Hs),* mouse *(Mus musculus,* Mm*), Xenopus laevis (Xl)* homeologs a and b, zebrafish *(Danio rerio, Dr)* and Starlet sea anemone *(Nematostella vectensis, Nv).* Shading indicates homology (black 80–100%, grey 60–80%). WW: WW domain, PRD: polar amino acid rich domain, NLS: nuclear localization signal, CTD: C-terminal conserved domain. The additional polar amino acid-rich tail highly conserved among species is marked by wavy line. **B.** Alignment of WBP11 protein sequences of human *(Hs),* mouse *(Mm), Xenopus laevis (Xl)* homeologs a and b, and *zebrafish (Dr).* Shading indicates homology (black 80–100%, grey 60–80%).

Fig. S2. Expression profile of *pqbp1* and *wbp11* mRNA during embryogenesis. Total RNA extracted from indicated developmental stages of *X. laevis* was used for qPCR analysis. The results were normalized to *ornithine decarboxylase* (ODC) levels and plotted relative to the level measured in the stage 35 embryos (set as 1.0).

Fig. S3. Expression of *pqbp1* and *wbp11* in neurula stage embryos. Whole mount *in situ* hybridization with indicated probes on embryos that were longitudinally sectioned (A) or cross-sectioned (B) stage 18 embryos. S: sense probe of *pqbp1*. Both *pqbp1* and *wbp11* transcripts are localized to ventro-lateral neural tube cells (B).

Fig. S4. Over-expression of PQBP1 inhibits normal specification and movement of dorsal mesoderm. Embryos at the end of gastrulation, stage 13, that had been dorsally injected at the 2-cell stage with 1 ng *pqbp1* mRNA, were analyzed by *in situ* hybridization with *brachyury* (*bra*) and *chordin* (*chd*) probes.

Fig. S5. Partial rescue of neural folding defects in PQBP1 morphants by *pqbp1* mRNA. A. PQ MO1 (40 ng) was dorsally injected with either 2 ng *b-galactosidase (b-gal*) or *pqbp1* (PQ) mRNA. **B.** Fraction of embryos displaying specific phenotypes: closed, partially closed or open neural folds (NF).

Fig. S6. *Xenopus* WBP11 interacts with PQBP1. A. Co-immunoprecipitation (co-IP) of PQBP1 and WBP11 from COS1 cells transfected with HA-tagged PQBP1 (HA-PQ) and myc-tagged WBP11 (myc-WB). Cell lysates were immunoprecipitated (IP) with an anti-myc antibody, followed by immunoblotting with an anti-HA antibody to detect PQBP1 bound to WBP11, or vice versa. TCL: total

cell lysate. **B**. Co-immunostaining of myc-tagged WBP11 (myc-WB) and HA-tagged PQBP1 (HA-PQ) expressed in COS1 cells. Nuclei were stained with DAPI.

Fig. S7. Validation of *pqbp1* knockdown effects on *fgf4* and *cdx4* expression in *X. laevis* and *X. tropicalis* embryos. Results were analyzed and plotted as described in Fig. 5. **A-C**. Expression of *fgf4* and *cdx4* was analyzed by qPCR. **A.** Either of the PQBP1 MOs (at 50 ng) reduced the expression of *fgf4* and *cdx4* in *X. laevis* morphant embryos, *P < 0.05 or **P < 0.01, with comparisons to control embryos (CT). **B.** Reduced *fgf4* and *cdx4* expression in embryos injected with 30 ng *pqbp1* MOb at the 4-cell stage into the VMZ was rescued by co-injection of MOb-resistant PQBP1 mRNA (0.4 ng or 2 ng) but not control *b-gal* mRNA (-); *P < 0.05 or **P < 0.01, with comparisons to MO-only injected embryos (-). **C.** Analysis of PQBP1 knockdown in *X. tropicalis* embryos. *X. tropicalis* PQBP1 MO (20 ng) was bilaterally injected into embryos at the 2-cell stage, and phenotypes of stage-matched wild type (WT) embryo (left panel) and MO-injected embryos (middle panel) are shown. Expression of *fgf4* and *cdx4* were evaluated in WT and *pqbp1* morphant *X. tropicalis* at the gastrula stage (right panel), as described in Fig. 5; *P < 0.05 or **P<0.01, with comparisons to control embryos (CT).

Fig. S8. Expression profile of different FGF receptors in Xenopus embryos. **A.** Total RNA was extracted from early neurula stage embryos, followed by Lightcycler qPCR (27 cycles) with each receptor-specific primer set, and amplification products were visualized by gel electrophoresis. **B.** Expression profile of FGF receptors in morphant gastrula stage embryos by qPCR. Samples were prepared and analyzed as per Fig. 5. Relative *fgfr* expression levels were calculated from the "crossing point" (CP) of qPCR cycle numbers for each primer set, using a common standard curve generated from *fgfr1IIIb* control embryo cDNA dilution series, and normalized to levels of *odc* transcripts. Bar graphs indicate the relative expression level of receptor transcripts in embryos injected with 150 ng control (CT), 100 ng *pqbp1* (PQ), 50 ng *wbp11* (BP), and combined *pqbp1* and *wbp11* (PQ+BP) MOs. Mean values for triplicate biological experiments are plotted; bars indicate standard error. Note, although expression levels of *fgfr1IIIc* and *fgfr3IIIb* transcripts appear nearly zero, they were detected in gel-based and qPCR.

Table S1. PCR Primers

Gene target		Primer sequence
odc	U	*GCCATTGTGAAGACTCTCTCC*
	D	TTCGGGTGATTCCTTGCCAC
wnt8	U	AGATGACGGCATTCCAGA
	D	TCTCCCGATATCTCAGGA
fgf4	U	CTTTCTTTCCAGAGAAACGACACCG
	D	AACTCACGACTCCAACTTCCACTG
fgf4 5'UTR	U	ACCTCCTCTGGGAGCTAAGCAGT
	D	TGGAAAGAAAGCGGCAGGCACT
cdx4	U	TCTCCTCATCCATCTGGGACTG
	D	AGTTCTGTCTTCCGCCTGATAGTG
fgf8	U	ATCACCTCCATCCTGGGCTATC
	D	TGCGAACTCTGCTTCCAAACG
brachyury	U	TTCTGAAGGTGAGCATGTCG
	D	GTTTGACTTTGCTAAAAGAGACAGG
siamois	U	CTGTCCTACAAGAGACTCTG
	D	TGTTGACTGCAGACTGTTGA
sizzled	U	CACACAAGACAGTCTTGGAAGCTTTC
	D	CACCAGCAATAACATACACTGTGGG
mix.2	U	TGCAAGCCATCATTATTCTAGC
	D	AGGAACCTCTGCCTCGAGACAT
apod (veg T)	U	TGGATTAGTTTAGGAACA
	D	CGGATCTTACACTGAGGA
sox2	U	GATCAGTATGTACCTACCTGG
	D	AGTGGAGAGCCACAGTTTGTC
chordin	U	AACTGCCAGGACTGGATGGT
	D	GGCAGGATTTAGAGTTGCTTC
noggin	U	AGTTGCAGATGTGGCTCT
	D	AGTCCAAGAGTCTGAGCA
goosecoid	U	TTCACCGATGAACAACTGGA

	D	TTCCACTTTTGGGCATTTTC
trop odc	U	ACAAGCTGTCTCAGATGCAC
	D	GCTCAGCAATGATGGTCACT
trop fgf4	U	GCAACGTGGGCATCGGGTTTCA
	D	TCCATACAGCTTCCCCTTTGCATTC
trop cdx4	U	AGCTGCCAACTCACCCAGCGAT
	D	TCCAGCTCCAGCCTCTGATGGT

Table S2. PCR Primers for FGFR

Gene target		**Primer sequence**
fgfr1 ex7	U	TGGCCTCGGATGGCTTCCCGTAT
fgfr1 ex8a	D	CGCAGACTGATTGGCCTCACCA
fgfr1 ex8b	U	TGGAGTTAGCGGCCAAGCAGGT
fgfr2 ex7	U	CCACATCCGCTGGGTGCGTTA
fgfr2 ex8a	D	TGCGTCCGCTTCGGTCACATT
fgfr2 ex8b	D	CCAGCATCCTCAAAAGAAACATTCCTG
fgfr2 ex8a	U	TCCAGTGCTGAAGTGCTGAAACTG
fgfr2 ex8b	U	ACATTCTGCCTGGTTGACGGT
fgfr2 ex9	D	TCTTCTTGGCTCCTTGCCGC
fgfr3 ex7	U	TGGCAGCAAGTACGGCCCAGA
fgfr3 ex8a	D	TGTCCTTCATGGGTCTCGGTCACA
fgfr3 ex8b	D	ACCGTCAGCCAAGCAGTGTGA
fgfr4 ex7	U	TGGAAGCCATTTTGGCCCTGATGA
fgfr4 ex9	D	TCTTGACTCTGCTGGCTCGGCT

Fig. S1

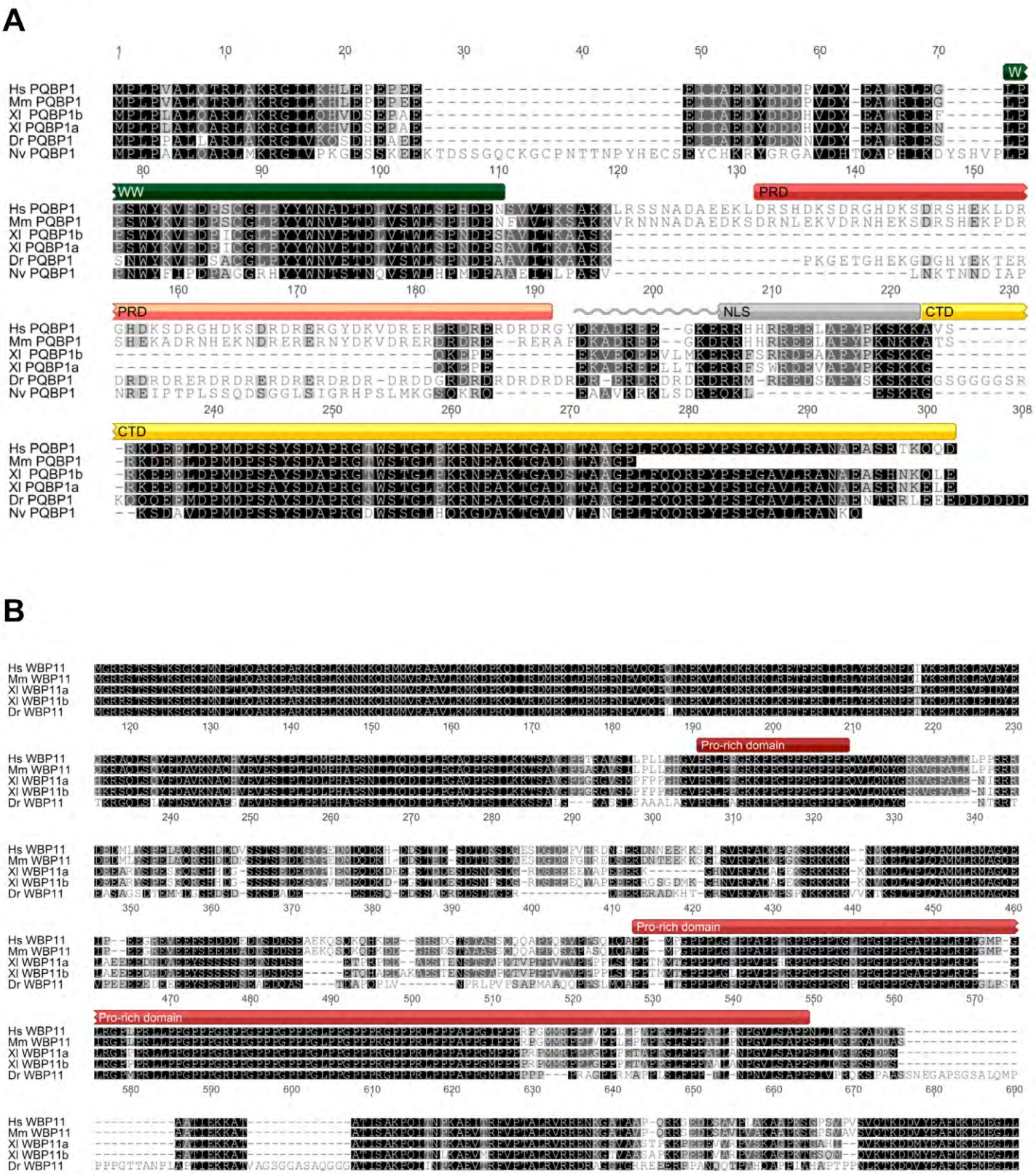
A
Hs PQBP1
Mm PQBP1
Xl PQBP1b
Xl PQBP1a
Dr PQBP1
Nv PQBP1
WW
PRD
NLS
CTD
B
Hs WBP11
Mm WBP11
Xl WBP11a
Xl WBP11b
Dr WBP11
Pro-rich domain

Fig. S2

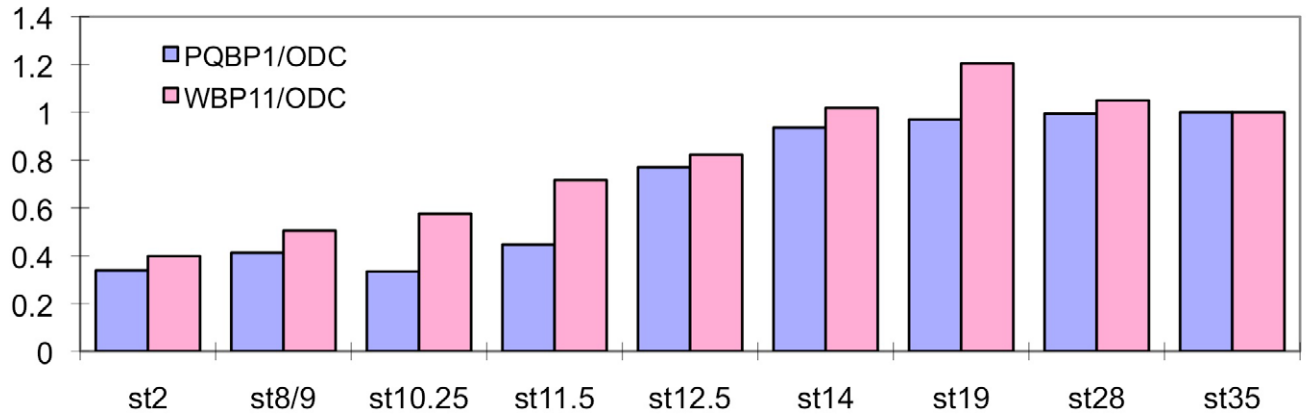
1.4
1.2
1
0.8
0.6
0.4
0.2
0
PQBP1/ODC
WBP11/ODC
st2
st8/9
st10.25
st11.5
st12.5
st14
st19
st28
st35

Fig. S3

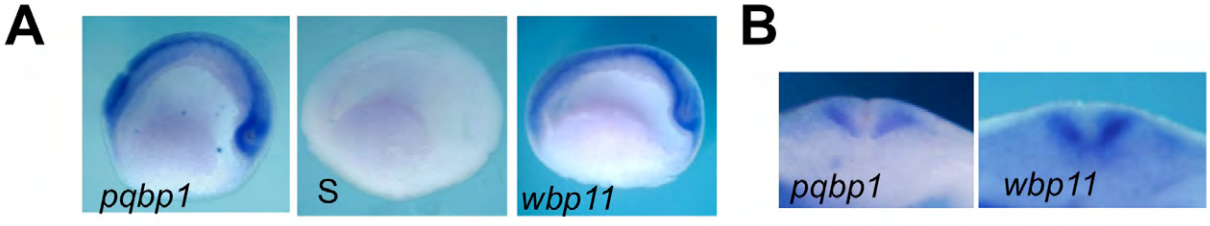
A
pqbp1
S
wbp11
B
pqbp1
wbp11

Fig. S4

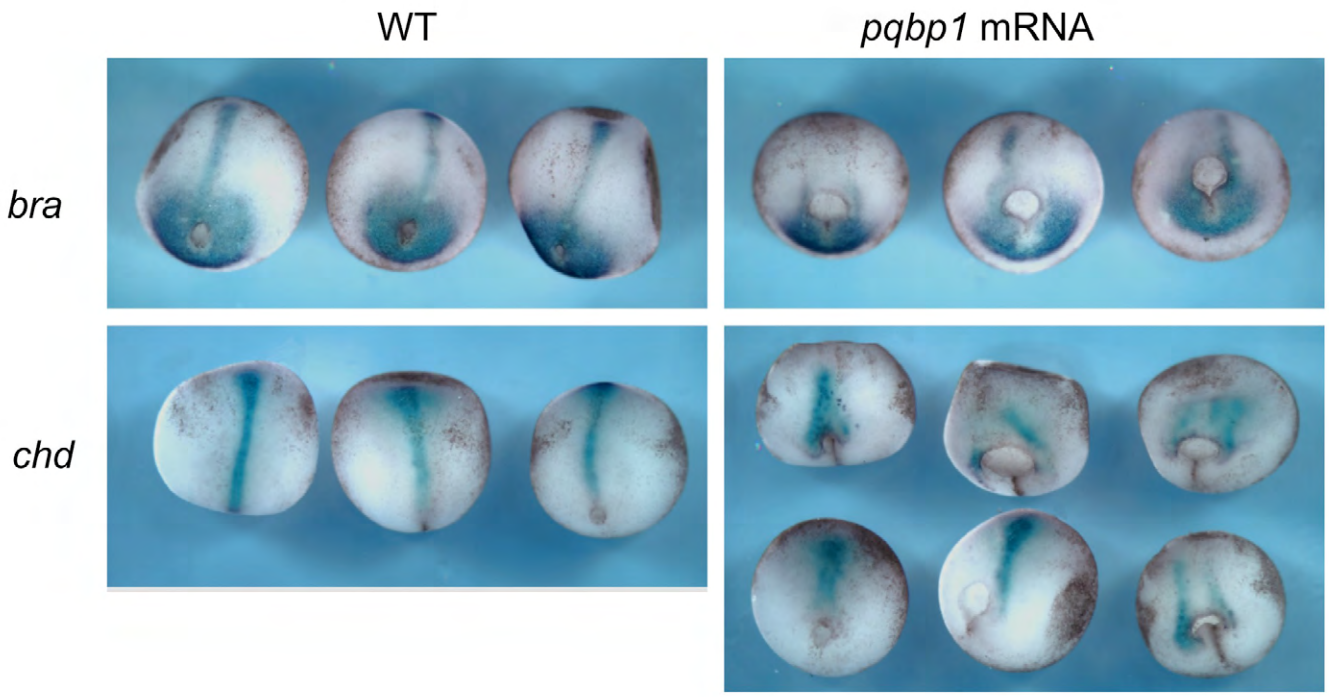

Fig. S5

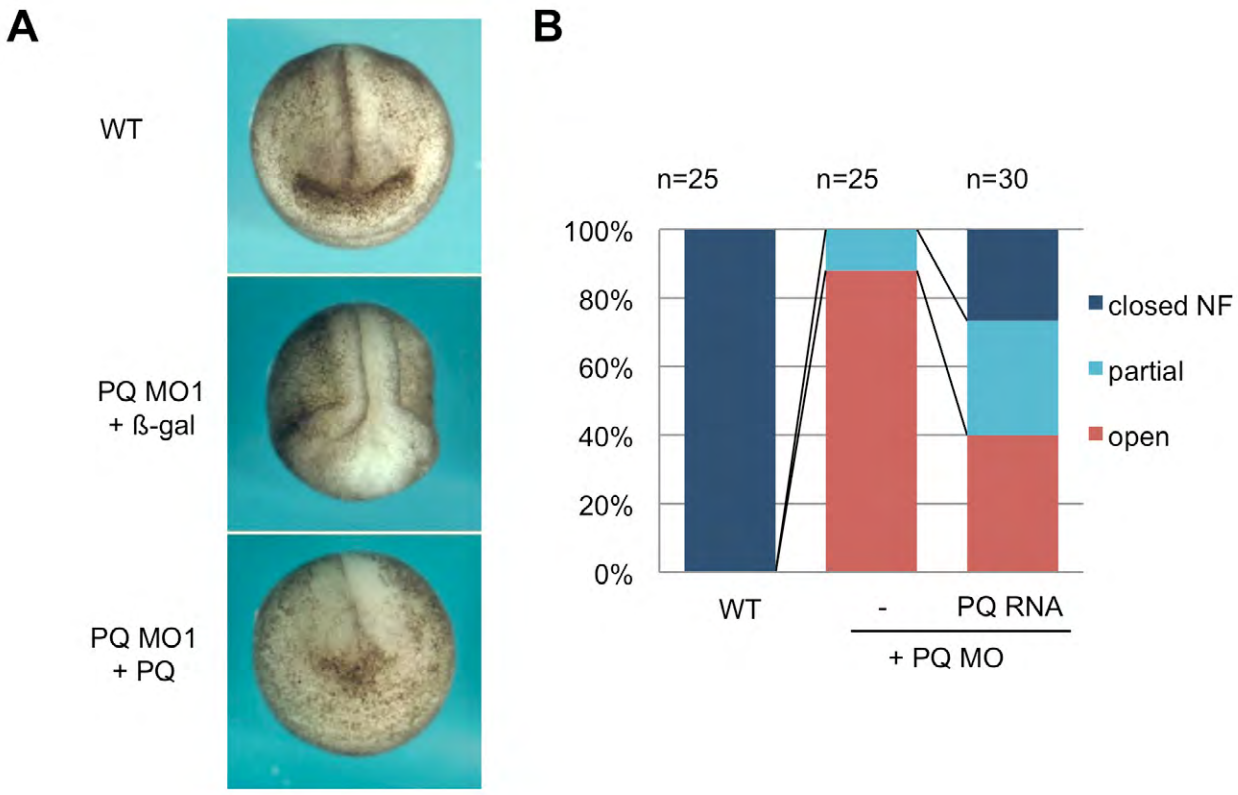
A
WT
PQ MO1
+ ß-gal
PQ MO1
+ PQ
B
n=25
n=25
n=30
100%
80%
60%
40%
20%
0%
closed NF
partial
open
WT
-
PQ RNA
+ PQ MO

Fig. S6

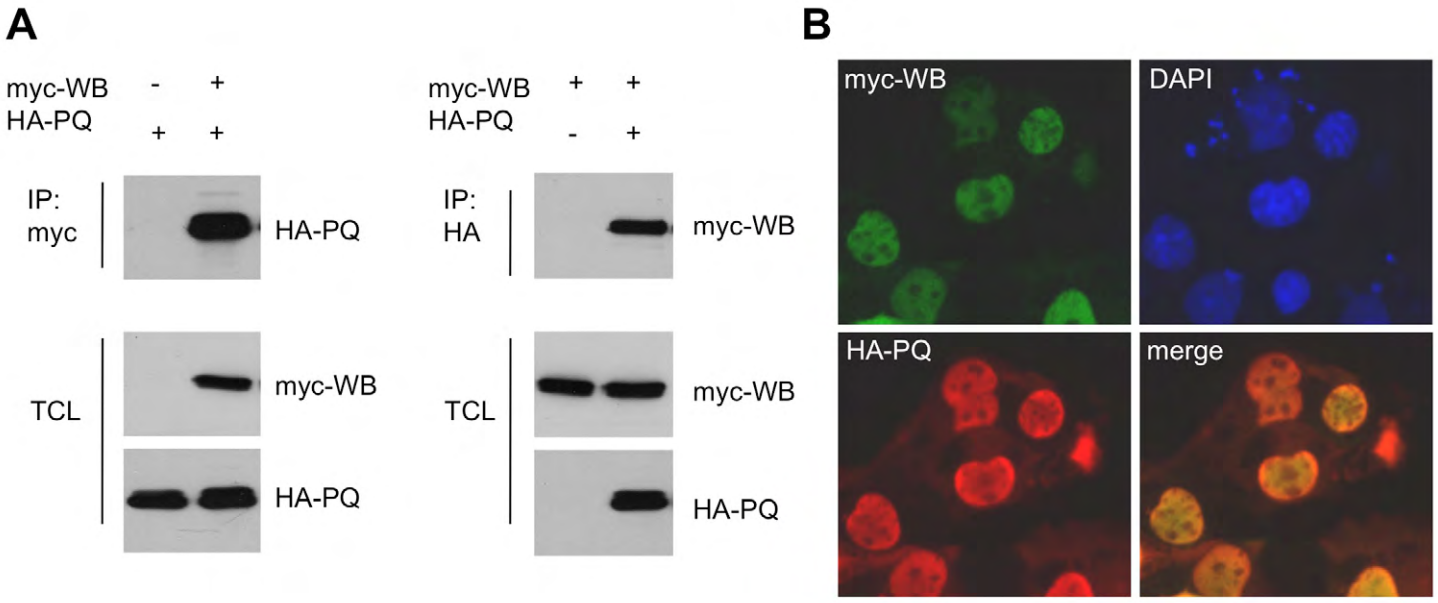
A
myc-WB - +
HA-PQ + +
IP: myc
HA-PQ
TCL
myc-WB
HA-PQ
myc-WB + +
HA-PQ - +
IP: HA
myc-WB
TCL
myc-WB
HA-PQ
B
myc-WB
DAPI
HA-PQ
merge

Fig. S7

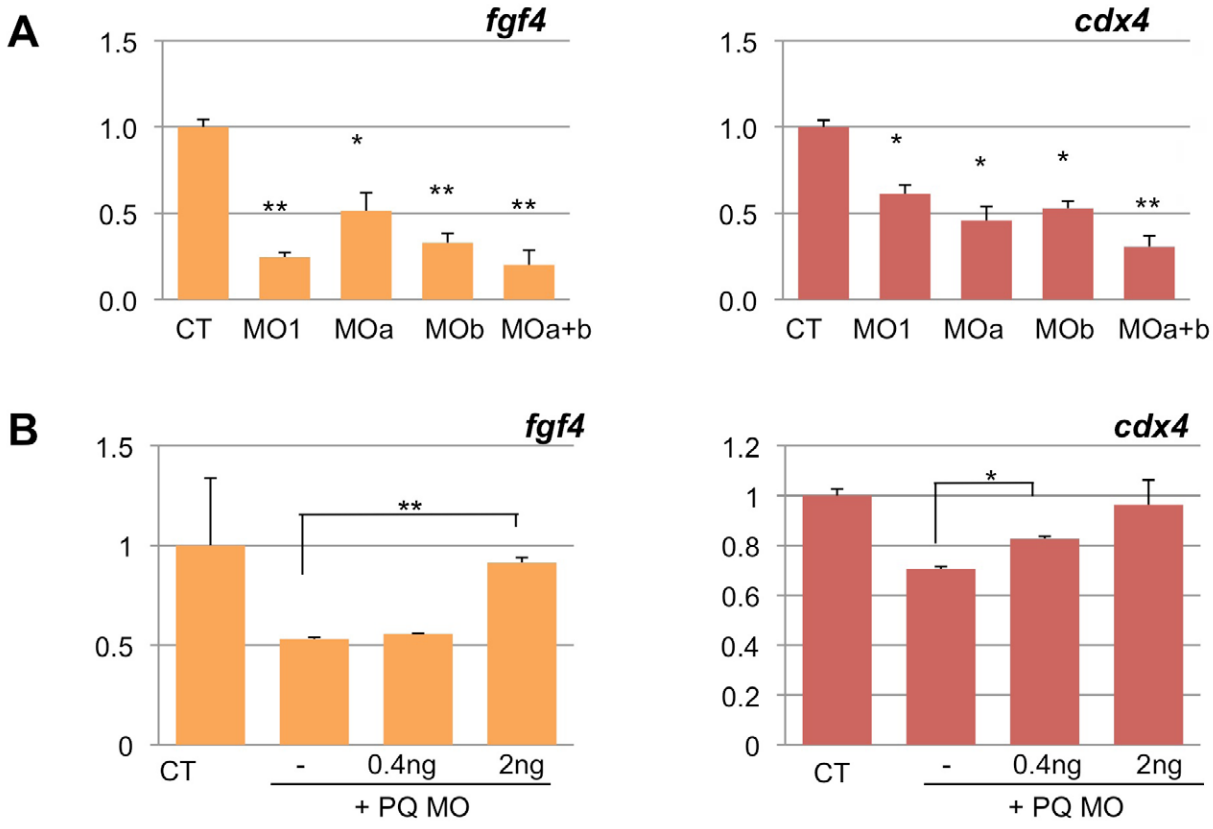
A
fgf4
1.5
1.0
0.5
0.0
CT
MO1
MOa
MOb
MOa+b
cdx4
B
fgf4
cdx4
CT
-
0.4ng
2ng
+ PQ MO

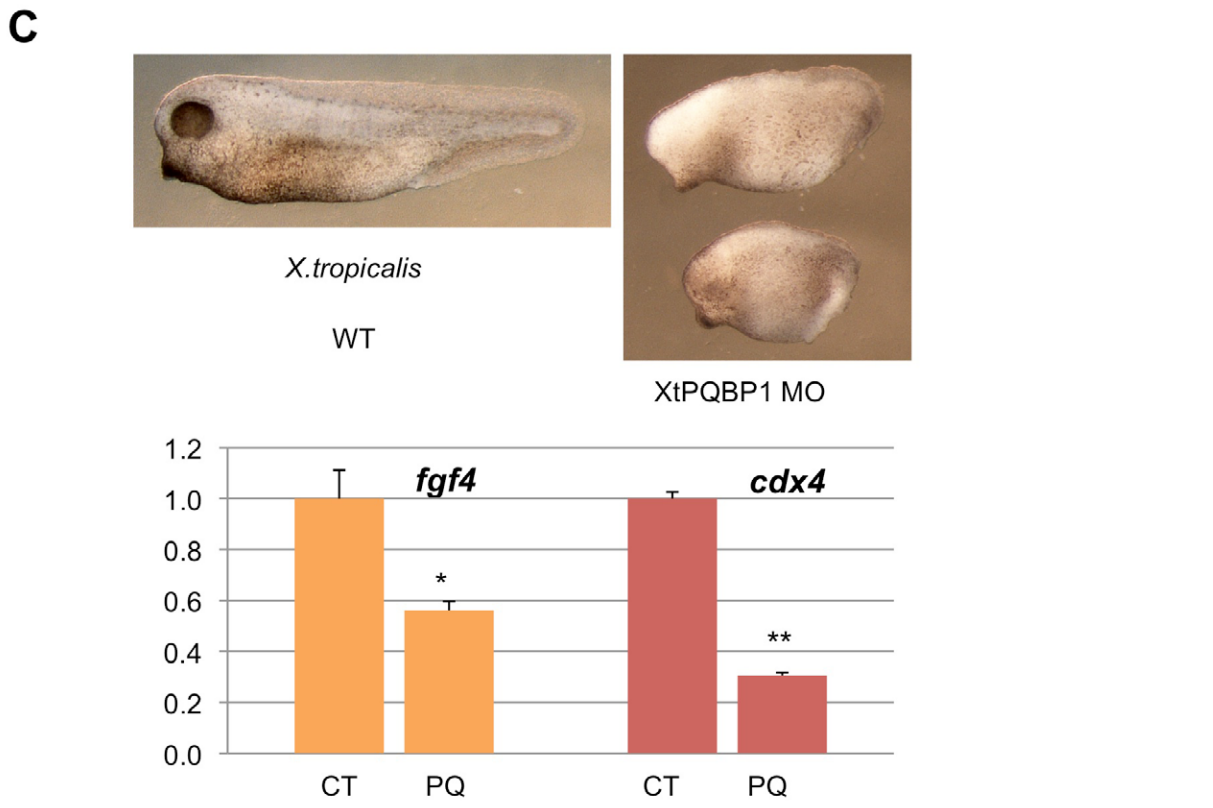
C
X.tropicalis
WT
XtPQBP1 MO
fgf4
cdx4
CT
PQ

Fig. S8

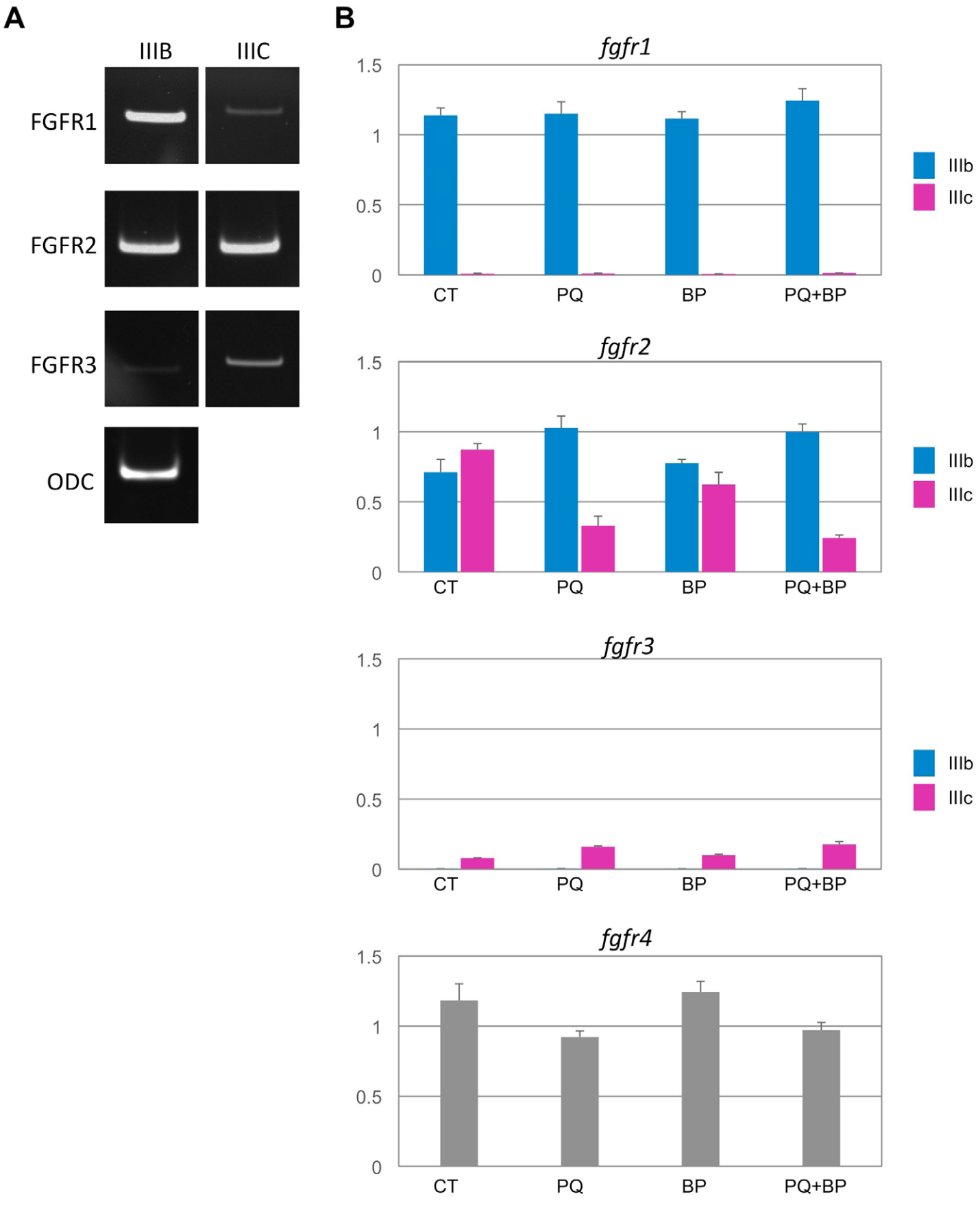
A
IIIB
IIIC
FGFR1
FGFR2
FGFR3
ODC
B
fgfr1
fgfr2
fgfr3
fgfr4
1.5
1
0.5
0
CT
PQ
BP
PQ+BP
IIIb
IIIc